

Scientific Spokesman:

W. F. Baker
National Accelerator Lab
P.O. Box 500
Batavia, Ill. 60510

FTS/Commercial: 312-840-3487

BACKWARD PION-PROTON ELASTIC SCATTERING

W. F. Baker, D. P. Eartly, P. Koehler, K. P. Pretzl*
S. M. Pruss and R. Rubinstein
National Accelerator Laboratory
Batavia, Illinois

and

R. M. Kalbach
University of Arizona
Tucson, Arizona

and

S. Mukhin
Joint Institute for Nuclear Research
Dubna, USSR

February 1974

*Present address Max Planck Institute, Munich

SUMMARY

The angular distribution of backward elastically scattered π^+ and π^- mesons from protons would be measured from 10 GeV/c to the maximum momenta possible. The apparatus would cover in one setting the full angular range from 90° to 180° in the laboratory, corresponding to $u > 0$ to $u \sim -0.8$ (GeV/c)². The directions and momenta of the incident pion, the scattered pion and the recoil proton would be measured with proportional wire chambers and analysis magnets.

Measurements at four incident momenta for each polarity would establish the energy dependence of the backward scattering angular distributions. It is estimated the 200 hours of testing time and 900 hours of data taking would be required to complete this study.

BACKWARD PION-PROTON ELASTIC SCATTERING

The purpose of this experiment is to measure the backward elastic scattering of π^+ and π^- mesons from protons at incident momenta from 10 GeV/c to the maximum possible. The angular range covered would extend from 90° to 180° in the laboratory, which corresponds to four-momentum transfers squared between the pion and proton from $u > 0$ to $u \sim -0.8$ (GeV/c)². The maximum momentum that can be reached cannot be accurately predicted until the discrepancies between theoretical predictions and presently available experimental data have been resolved.

PHYSICS JUSTIFICATION

Backward pion-nucleon elastic scattering has been measured from intermediate momenta up to 40 GeV/c in a number of experiments.¹⁻⁶ At these momenta baryon exchange processes are believed to dominate the reactions. At lower momenta, below ~ 5 GeV/c, studies of the energy dependence of both $\pi^+ - p$ and $\pi^- - p$ backward scattering^{6,7} show structure that can be interpreted in terms of direct channel baryon resonances. At higher energies such structure is not expected.

The Regge formalism has successfully described some of the features of backward scattering at high energies. The now well-known dip in π^+p scattering at $u = -0.15$ (GeV/c)² is explained as the passage of the

N_α trajectory through a singularity at $-1/2$. The energy dependence is of the form: $s^{2\alpha_{\text{eff}}-2}$ where α_{eff} is the effective Regge trajectory. A review of the various theories of backward πN scattering has been given by Berger and Fox.⁸

The energy dependence of the differential cross section $d\sigma/du$ at $u = 0$ is given in Figure 1. The points of Babaev, et al⁵ are for backward π^- -neutron scattering and should be compared with the π^+p points at lower energy. A visual fit of the Regge form to these data yields an energy dependence of $\sim s^{-1.7}$ ($\alpha_{\text{eff}} = 0.15$). This is in strong disagreement with the various Regge theories which require an $\alpha_{\text{eff}} < 0$. Hayot⁹ has predicted angular distributions and the energy dependence expected at NAL energies. His curve for π^+p is shown as $s^{-2.7}$ ($\alpha_{\text{eff}} = -0.35$) and for π^-p as $s^{-2.0}$ ($\alpha_{\text{eff}} \approx 0$).

Angular distributions are shown in Figure 2. The 10 GeV/c curves are fits to the data of Owen, et al.⁴ The 50 and 100 GeV/c curves are the predictions of Hayot.⁹

As both N and Δ exchange can contribute to π^+p backward scattering one could attempt to explain the observed energy dependence above 10 GeV/c as the Δ exchange becoming dominant. If this were the case one would expect the slope of the backward peak to be less steep than at lower energies and comparable to the slope for π^-p scattering, which is due to Δ exchange only. Babaev, et al⁵, however, at 40 GeV/c see a steep backward

peak with a slope of $B = 26 \pm 6 \text{ (GeV/c)}^{-2}$ in fitting to $d\sigma/du = A \exp (Bu)$, whereas with Δ exchange alone one would expect $B \sim 6 \text{ (GeV/c)}^{-2}$.

Theory leads us to expect several interesting phenomena:

1. The π^-p backward ($u = 0$) cross section should become larger than the π^+p cross section,
2. The π^+p backward peak should show antishrinkage as the Δ exchange becomes more dominant,
3. The secondary maximum at $u = -0.5 \text{ (GeV/c)}^2$ should drop away, similar to the behavior seen in forward scattering. The dip will move out in $|u|$ also.

If the energy dependence shown by the existing data, Figure 1, which violates a simple prediction proves to be correct, however, then the predictions for the angular distributions could also be wrong. The s and u dependences are intrinsically coupled. Therefore, a systematic examination of them both is very important.

While measuring πp events we would also be sensitive to backward Kp elastic scattering. K^+p backward peaks have been measured up to 7 GeV/c^2 . An energy dependence, at $u = 0$, of s^{-4} is indicated which is consistent with a linear extrapolation of the $\Lambda_\alpha - \Lambda_\gamma$ trajectories. This predicts $d\sigma/du \sim 1 \mu\text{b}/(\text{GeV/c})^2$ at 10 GeV/c . At lower energies K^-p backward scattering is observed to drop much faster with energy, as expected, and would therefore be more difficult to detect. In any case kaon fluxes would be

low, and although we would detect Kp backward scattering, this measurement would not be the primary goal of the experiment.

EXPERIMENTAL METHOD AND EQUIPMENT

A comparison of Figures 1 and 2 shows that whereas $d\sigma/du$ is a monotonic function of s at these energies, it is a considerably more complex function of u . We have, therefore, chosen a geometry which will cover the full u range in one setting. In fact, the backward, or u -determining, arm would not be changed throughout the experiment. We feel that this is essential to reduce biases and systematic errors to an absolute minimum and to make u structure fully believable. History bears out this feeling; although several experiments had been done on backward scattering, the existence of the dip at $u = -0.15 \text{ (GeV/c)}^2$ in π^+p was not definitively established until one geometry covered the complete dip region.

The geometry chosen for this experiment is shown in Figures 3 and 4. The angle of the scattered pion for a given value of u is essentially independent of incident pion momentum at these energies.¹⁰ The backward arm, Figure 3, would therefore remain fixed throughout the experiment. The angle of the forward going recoil proton, however, scales inversely with momentum for a given u , thus the forward arm, Figure 4, would be lengthened proportionately with energy.

A 40" (1 meter) long liquid hydrogen target is chosen as a good match to the magnet selected for the backward arm.

The magnet would be roughly similar to the 72D18 magnets in use at Brookhaven. Such a magnet would have a pole tip ~ 18 " long and would be opened to 18 ". This permits an approximate match to the azimuthal acceptance of the forward arm, and allows the incident beam to clear the coils through a hole in the return yoke. The bending power is taken as 7 kilogauss-meters.

The wider the magnet the larger the range of u that can be covered. The figure shows a pole tip width of 96 ". With this width, scattering from the entire length of the target can be observed from $u > 0$ out to the peak of the secondary maximum (in π^+p) at $u = -0.5 \text{ (GeV/c)}^2$. Beyond this point the effective target length decreases. An ideal magnet would be ~ 120 " wide; such a magnet would extend the range of a fully effective target length over the secondary maximum to $u \sim -0.8 \text{ (GeV/c)}^2$. With a 72D18 the effective target length drops to one-half at $u = -0.5 \text{ (GeV/c)}^2$. Thus the extent of the u range covered will be determined by the width of the magnet made available to us.

The direction of the scattered pion would be determined by proportional wire chambers preceding the magnet. These chambers, in conjunction with those following the magnet would establish the pion's momentum. The latter would only have vertical wires with larger spacings (~ 5 mm). The resultant momentum resolution of a few percent is adequate to distinguish the forward going recoil proton from a nucleon resonance. The track recognition and reconstruction programs would include the deflection in

the magnetic field. A fence of scintillation counters S_B are used in the event trigger. Anticounters would be placed near the target to reduce background.

The forward arm, Figure 4, uses two NAL 24D72 (BM109) analysis magnets. These magnets have a geometric aperture which matches the backward arm and yield the requisite momentum resolution for the forward proton. The direction of the proton is determined by proportional wire chambers between the target and the magnets. The chambers following the magnets would again have only vertical wires and with 2 mm wire spacing would yield a momentum resolution of $\pm 0.2\%$. At 70 GeV/c this is equivalent to one pion mass and is one-third of the amount by which the recoil proton momentum exceeds the momentum of the beam and forward scattered particles.

The threshold Cerenkov counter, \bar{C} , is set well above the pion threshold but below that for protons. This is placed in anticoincidence to reduce the number of triggers from forward scattering. At higher momenta, where the arm is adequately long this counter would precede the final chambers, at lower energies it would follow them. This counter would be about four feet in diameter and could be similar to other counters that have been or are being built, although requirements on its resolution are less stringent, i.e., it is not required to separate kaons from pions. Gaps in the forward arm would be filled with helium bags. The scintillation counter fence, S_F , is used in the event trigger.

The forward arm would be scaled such that each leg, preceding and following the magnets, would have a length of approximately $1.5 P_0$ feet; with P_0 the incident beam momentum in GeV/c. All components of this arm could be mounted on a cart and rail system similar to that in the M1 beam line.

Experience tells us that resolving times of 200 ns are readily obtainable with proportional wire chambers. Having the beam spread over ten wires thus allows beam intensities of 5×10^6 /sec if 10% accidentals are permitted. For this reason we intend to let the incident beam pass through some of the chambers.

Mass definition of the incident particle would be accomplished with Cerenkov counters which we assume to exist in the beam line. Momentum definition of the incident particle would be established with a hodoscope located at a momentum dispersed focus. This definition would be comparable to that of the forward arm. Proportional wire chambers preceding the target would establish the incident trajectory.

In our original letter of intent of June 1970 we proposed using focusing elements in the forward arm as was done in the experiment of Reference 6. These would permit the use of detectors of smaller area with a resultant cost saving. However, as the requisite quadrupole magnets do not exist at NAL, we conclude that it would be more economical to use the configuration of Figure 6. A focusing forward arm would be of variable length also.

An on-line computer of the PDP-11 or PDP-15 type would be required for buffering and recording data and for real-time diagnostics.

As the participants in this experiment would mostly be NAL staff members, it is expected that NAL would supply most of the equipment. However, except for a few specialized items it already exists. The University of Arizona could contribute in the fabrication of wire chambers and scintillation counters. A liquid hydrogen target is required with a single thin window along its entire side and upstream end.

A modest amount of standard fast electronics would be required from PREP to provide the triggering logic.

Event reconstruction and data reduction could be done either on-line or off-line depending on the available computer situation at NAL at the time.

INELASTIC BACKGROUNDS

Although inelastic background calculations are notoriously unreliable, we can nevertheless obtain a reasonable background estimate from our experience in previous similar experiments.

That the background is approximately constant in u can be seen from one of the Cornell-BNL experiments⁴ at 6-17 GeV/c. In one arrangement the momentum and angle of the scattered pion were measured with only crude information on the proton. The background was $\sim 1\%$ at $u = 0$, increasing to $\sim 40\%$ near $u = -1.5$ (GeV/c)², while the signal decreased by a factor of ~ 40 in this range.

An on-line computer of the PDP-11 or PDP-15 type would be required for buffering and recording data and for real-time diagnostics.

As the participants in this experiment would mostly be NAL staff members, it is expected that NAL would supply most of the equipment. However, except for a few specialized items it already exists. The University of Arizona could contribute in the fabrication of wire chambers and scintillation counters. A liquid hydrogen target is required with a single thin window along its entire side and upstream end.

A modest amount of standard fast electronics would be required from PREP to provide the triggering logic.

Event reconstruction and data reduction could be surprising in that all of these reactions are due to baryon exchange.

Even at larger $|u|$ the background constancy appears to hold. The Cornell-BNL group found that out to $u = -2 \text{ (GeV/c)}^2$ backgrounds were only 10-50%. The geometry was slightly different at these angles, only directions of outgoing particles after magnetic deflection were measured; thus again there were fewer constraints than we are proposing.

We therefore conclude that the background in the final event distributions of our experiment is readily manageable at least up to 40 GeV/c and, assuming the ratios to hold, to higher energies.

DATA RATES

The sensitivity of this apparatus and the expected

data rates are based on the following assumptions: a one-meter long liquid hydrogen target, 5×10^6 pions/burst and 1000 bursts/hour. Particle production studies¹¹ in the M1 beam indicate that such intensities are obtainable, in the energy range of interest, with $1-2 \times 10^{12}$ protons of 300 GeV energy on the production target. As protons do not represent a major fraction of the positive secondary beam, in this range, the sensitivity of the overall system can be taken as energy independent.

Thus the expression for the number of events per hour:

$$N = N_0 \ell \rho A_0 \frac{d\sigma}{du} \cdot \Delta u \cdot \epsilon_\phi$$

becomes:

$$N = 21 \cdot \Delta u \cdot \epsilon_\phi \cdot \frac{d\sigma}{du}$$

where Δu is the bin width in $(\text{GeV}/c)^2$, ϵ_ϕ is the fraction of total azimuth accepted and $\frac{d\sigma}{du}$ is the differential cross section in nanobarns/ $(\text{GeV}/c)^2$.

The sensitivity as a function of u is given in Table 1 for three possible recoil magnet widths.

We have calculated the expected data rates assuming the shapes of the angular distributions to have the energy dependences shown in Figure 2. We then make various assumptions regarding the energy dependence of the magnitude of the cross sections at $u = 0$. The recoil arm magnet is taken as a 96D18.

At 10 GeV/c we take the curves of Figure 2 which are fits to the data of Owen, et al⁴. We have taken the

theoretical predictions of Hayot⁹ at 50 GeV/c and 100 GeV/c. For π^+p this implies an $s^{-2.7}$ energy dependence and for π^-p an $s^{-2.0}$ energy dependence. The models reviewed by Berger and Fox⁸ predict a similar energy dependence for π^+p , but a steeper drop-off for π^-p . We have also drawn a straight line best fit to the π^+p data, without regard for theories, and find an $s^{-1.7}$ energy dependence. We have calculated data rates from this and find them an order of magnitude higher at 100 GeV/c than the theories predict.

The following table gives the data rates per hour under these various assumptions. The bins of the previous table are retained.

The experimental program we would follow would be partially determined by preliminary results. We would first repeat one of the energies measured at Brookhaven⁴ to test the apparatus at reasonably high data rates. We would then investigate the energies used at Serpukhov⁵ for π^-n scattering. If the energy dependence indicated by that data is borne out, we could extend our measurements to higher energies than would be possible with the faster drop-off with energy predicted by theory. Studies as high as 100 GeV/c and above would be possible. With the faster drop-off, 70 or 80 GeV/c would probably be the maximum energy. To run at three or four energies for each polarity, we would require about 900 hours of good data taking beam; an additional 200 hours would be required for testing.

The large angular acceptance of this apparatus, particularly of the backward arm, permits a study of other baryon exchange processes than elastic scattering. Because of this acceptance our tapes would include data on such reactions as backward ρ production and forward baryon resonance production. We would hope to extract this interesting physics.

FUTURE POSSIBILITIES

A future step in a program to study backward scattering would be an examination of polarization effects. The development of frozen polarized targets would facilitate this with few changes in the proposed apparatus.

A more thorough investigation of backward Kp scattering would best be conducted with this apparatus in a secondary beam of minimal length and with more modest energy requirements than for πp scattering.

REFERENCES

- ¹J. Orear, et al, Phys. Rev. 152, 1162 (1966).
- ²W. F. Baker, et al, Phys. Lett. 28B, 291 (1968);
K. P. Pretzl, Thesis, University of Munich (1968),
and private communication.
- ³E. W. Anderson, et al, Phys. Rev. Lett. 20, 1529 (1968).
- ⁴D. P. Owen, et al, Phys. Rev. 181, 1794 (1969),
and D. P. Owen, Thesis, Cornell University (1969).
- ⁵A. Babaev, et al, Phys. Lett. 38B, 342 (1972).
- ⁶W. F. Baker, et al, Phys. Rev. Lett. 32, 251 (1974)
and private communication.
- ⁷S. W. Kormanyos, et al, Phys. Rev. Lett. 16, 709 (1966).
- ⁸E. L. Berger and G. C. Fox, Nuclear Physics B26, 1
(1971).
- ⁹F. Hayot and G. Kane, private communication; see also
F. Hayot and A. Morel, Phys. Rev. D8, 223 (1973).
- ¹⁰R. M. Kalbach, Two Body Kinematics 10-1000 GeV, NAL
Batavia (1973).
- ¹¹W. F. Baker, et al, NAL-Pub-71/13-EXP 7100.104, and
submitted to Phys. Rev. Lett.

TABLE 1

Sensitivity of System as a Function of u

\bar{u} $(\text{GeV}/c)^2$	Δu $(\text{GeV}/c)^2$	Sensitivity ($21 \cdot \Delta u \cdot \epsilon_\phi$) $\frac{(\text{GeV}/c)^2}{\text{nb-hr}}$		
		<u>120D18</u>	<u>96D18</u>	<u>72D18</u>
-0.025	.05	.17	.17	.17
-0.075	.05	.11	.11	.11
-0.125	.05	.10	.10	.10
-0.175	.05	.08	.08	.08
-0.25	.10	.15	.15	.15
-0.35	.10	.13	.13	.10
-0.50	.20	.24	.24	.12
-0.70	.20	.20	.13	.03
-0.90	.20	.18	.09	.00

TABLE 2

np Elastic Backward Scattering Event Rates

P_0 (GeV/c) Energy Dependence \bar{u} (GeV/c)	+10	-10	+50	+50	-50	+100	+100	-100
	Data Fit	Data Fit	$S^{-2.7}$ Hayot	$S^{-1.7}$ Data Fit	$S^{-2.0}$ Hayot	$S^{-2.7}$ Hayot	$S^{-1.7}$ Data Fit	$S^{-2.0}$ Hayot
-0.025	370	286	6.7	33.5	10.4	0.89	8.9	2.52
-0.075	66	145	1.3	6.5	4.2	0.21	2.1	1.00
-0.125	15	95	0.4	2.0	2.7	0.08	0.8	0.57
-0.175	16	63	0.1	0.5	1.5	0.03	0.3	0.27
-0.25	60	79	0.2	1.0	1.5	0.03	0.3	0.23
-0.35	80	42	0.2	1.0	.6	0.02	0.2	0.08
-0.50	170	35	0.6	3.0	.3	0.06	0.6	0.03
-0.70	60	8	0.3	1.5	.04	0.03	0.3	0.01
-0.90	18	2	0.2	1.0	.01	0.02	0.2	--
Total Events Per Hour	855	755	10	50	21	1.4	14	4.8

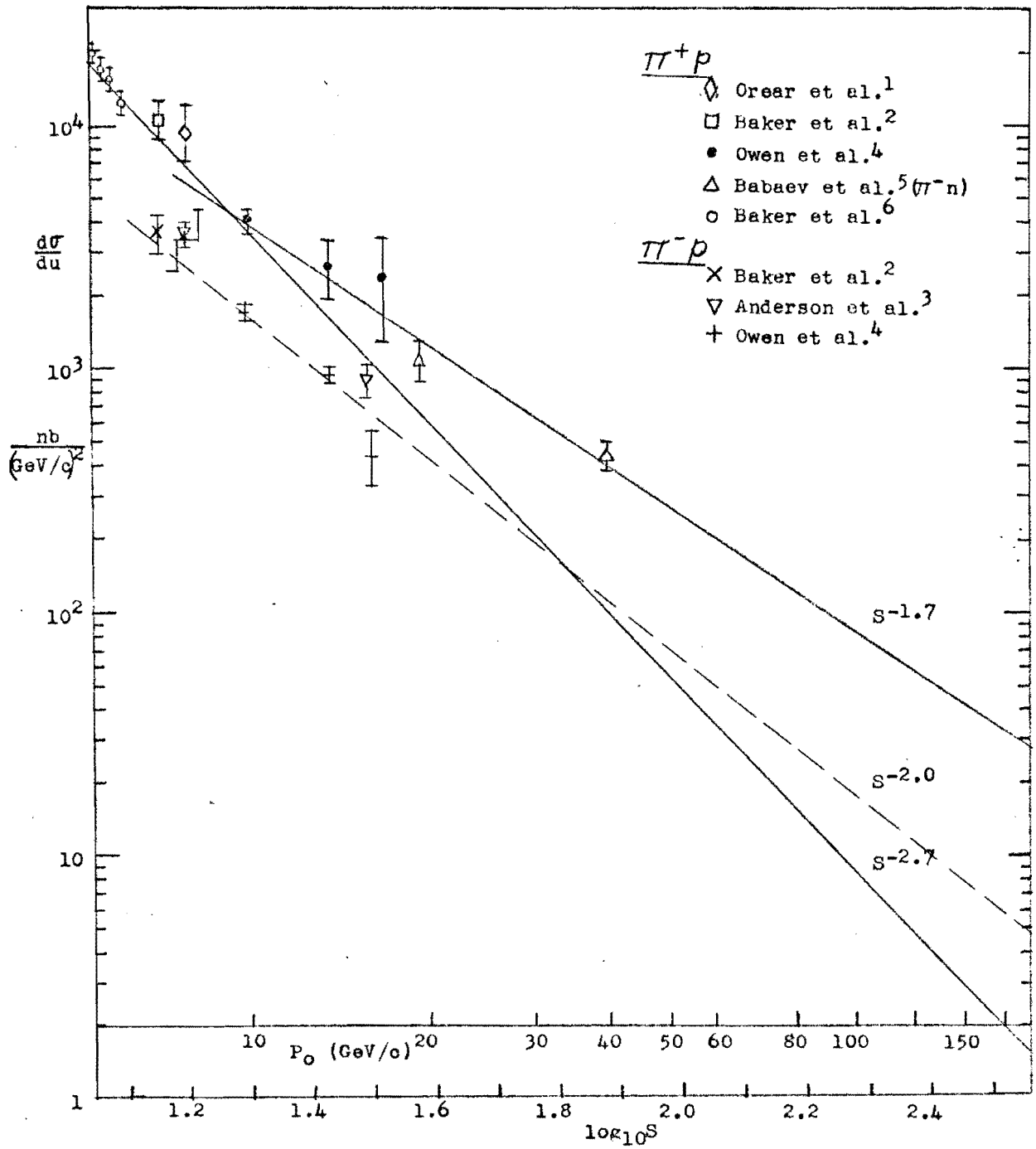


FIG. 1. The energy dependence of backward π -p scattering at $u = 0$.

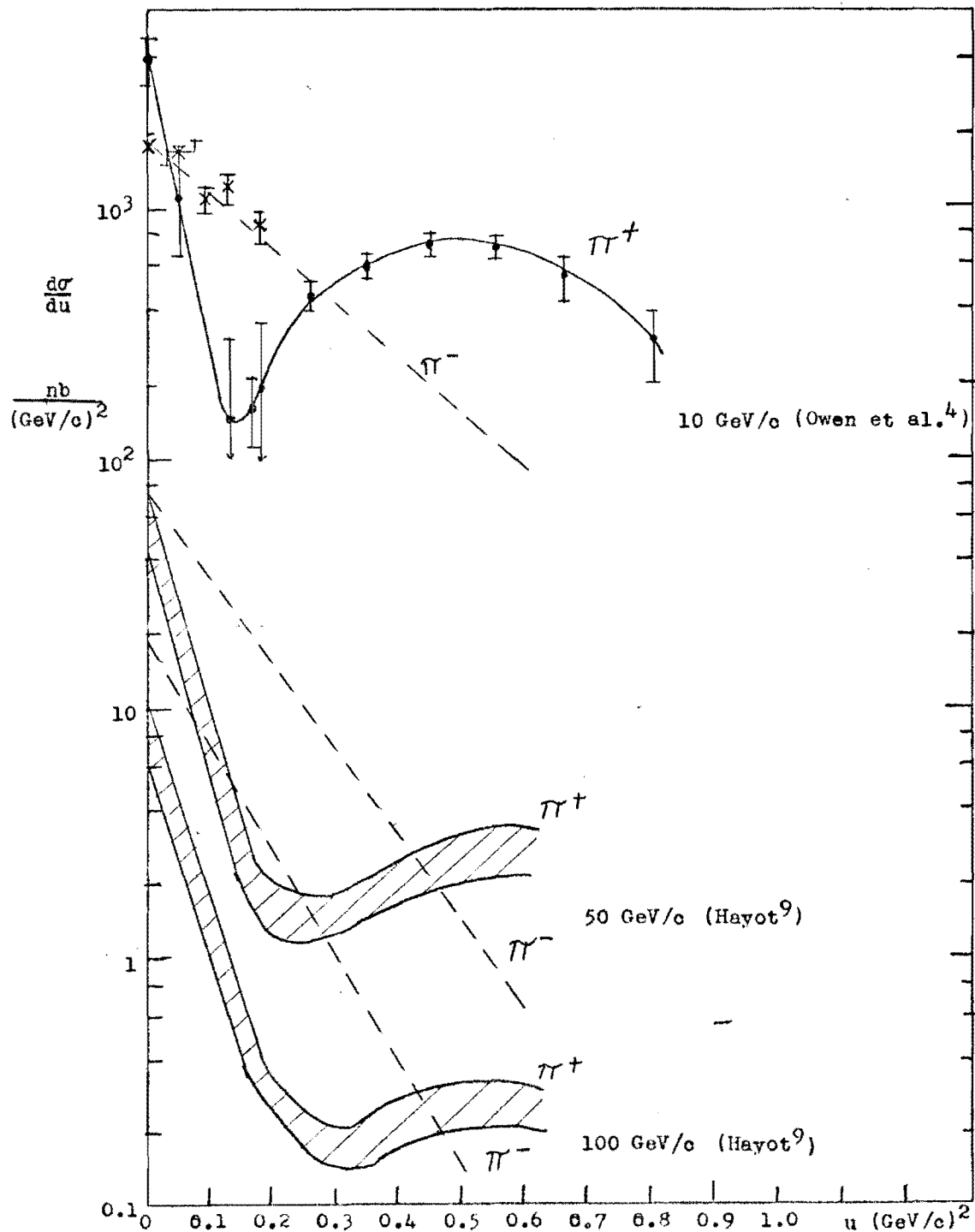


FIG. 29. The angular distributions of backward π -p scattering.

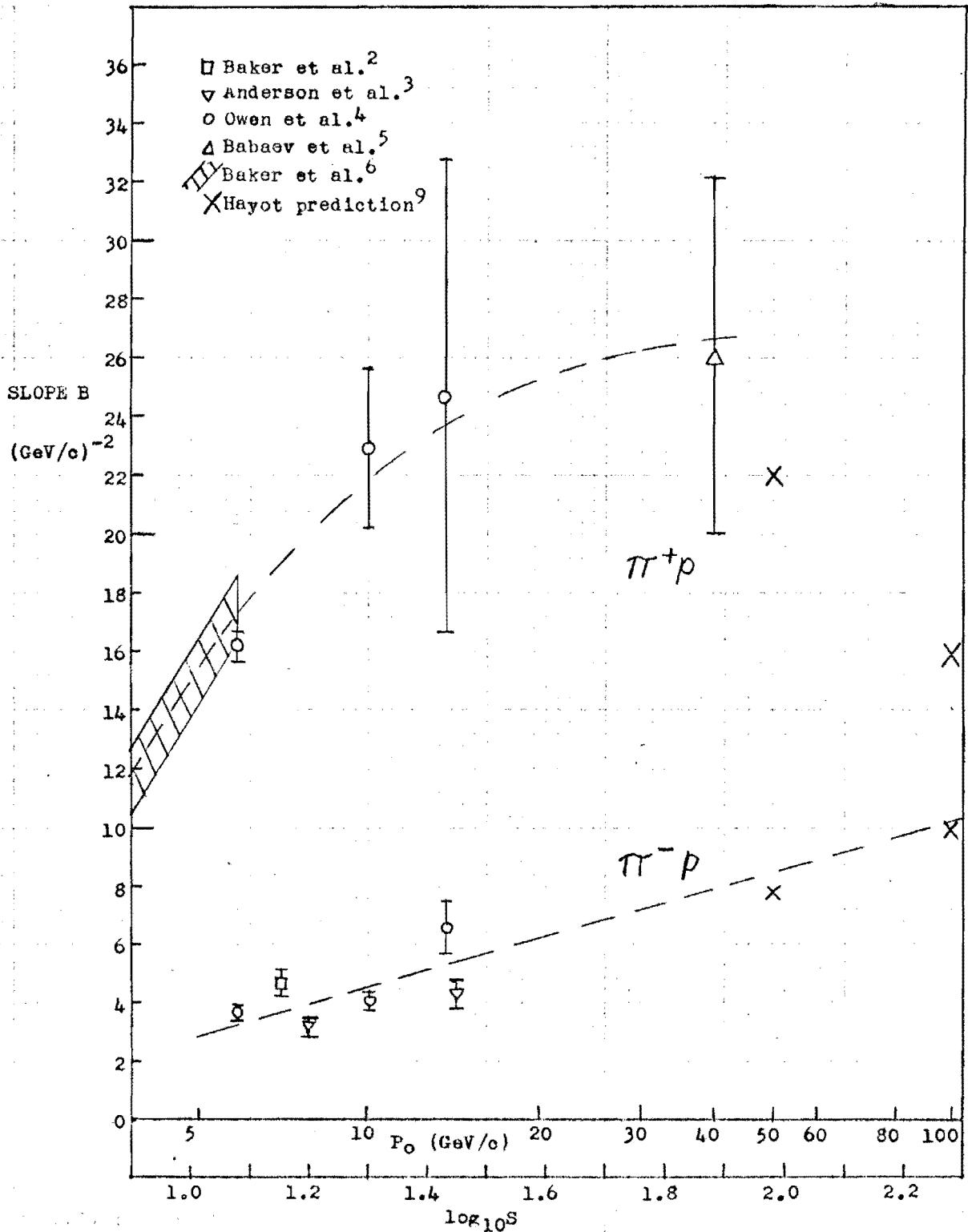


FIG. 2b. The slope of the backward peak in πp scattering as a function of energy. The cross hatched region represents 20 data points from ref. 6. The slope parameter B is from a fit to the form $A \cdot \exp(Bu)$. The dashed lines are to guide the eye.

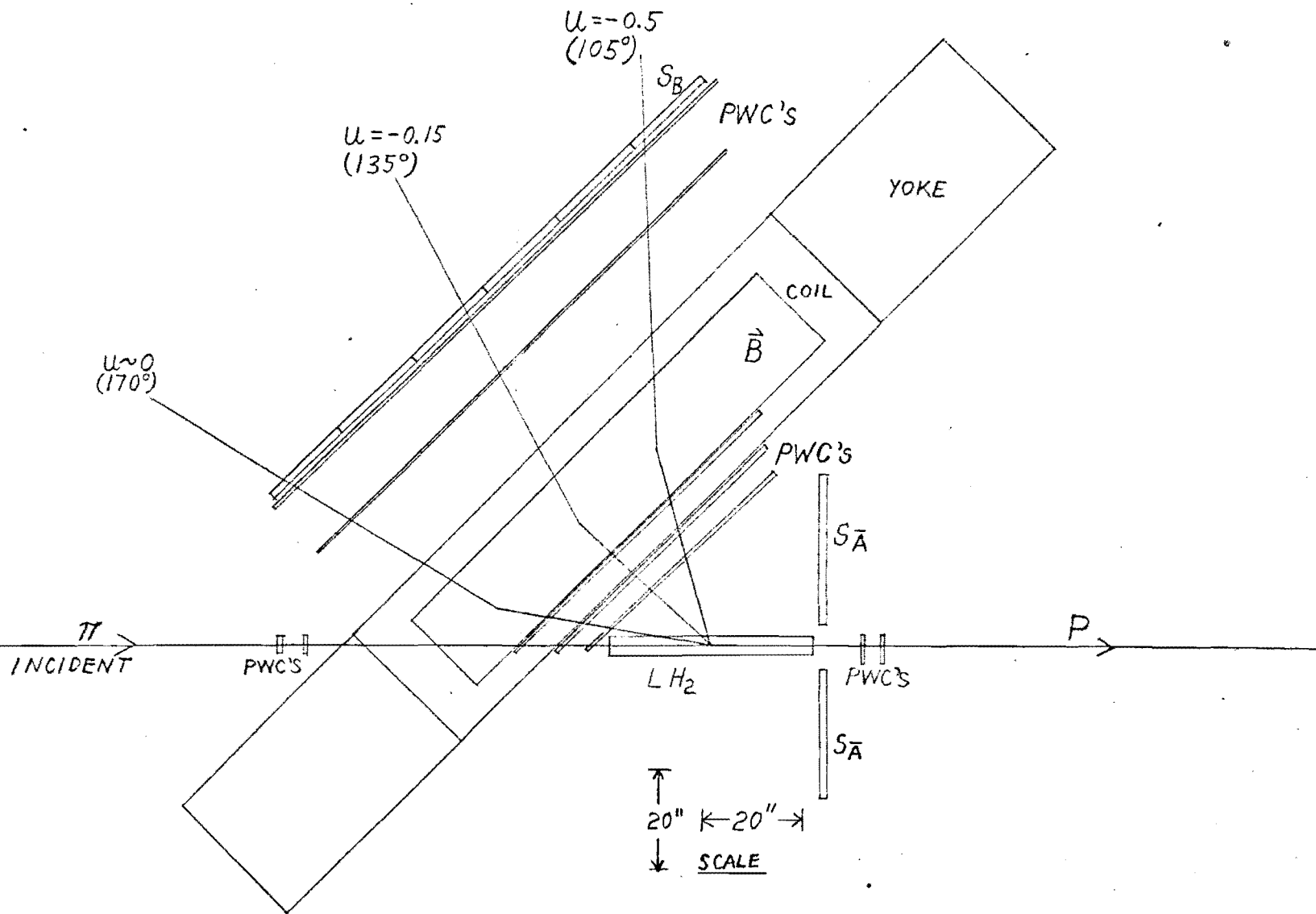


FIG. 3. BACKWARD ARM CONFIGURATION FOR ALL MOMENTA

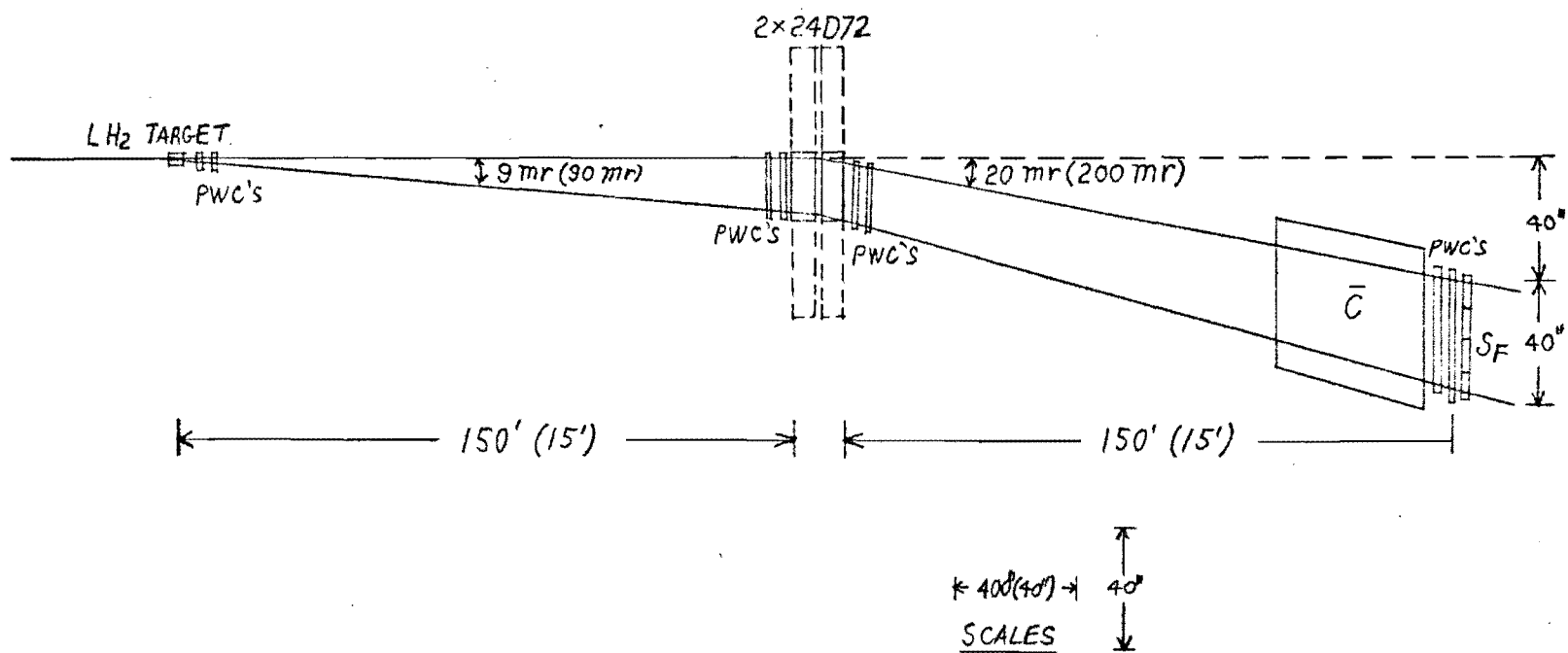


FIG. 4. FORWARD ARM CONFIGURATION FOR 100 GeV/c (10 GeV/c) OPERATION